J Toxicol Pathol 2021; 34: 299–308

Original Article

Time-course changes in 5-fluorouracil-induced neural progenitor cell damages in the developing rat brain

Yuko Yamaguchi[1]*, Yachiyo Fukunaga[1], Mizuho Takagi[1], Tsubasa Saito[1], Kazutoshi Tamura[1], and Toru Hoshiya[1]

[1] Pathology Division, Gotemba Laboratories, BoZo Research Center Inc, 1284 Kamado, Gotemba, Shizuoka 412-0039, Japan

Abstract: 5-Fluorouracil (5-Fu) is a DNA-damaging agent and teratogenic in rodents. This study aimed to investigate its influence on neural progenitor cells (NPCs) in the developing fetal rat brain. Dams were intraperitoneally injected with 5-Fu (50 mg/kg b.w.) on gestation day 13 and its effects on fetal NPCs were observed from 3 to 72 hours after treatment (HAT), via periodic examination at six intervals. In NPCs of the fetal brain, the p53-labeling index (LI%) was markedly elevated at 3 HAT. Pyknosis and cleaved caspase-3-LI% also increased at 3 HAT, reaching peak values at 9 and 12 HAT. These parallel changes suggested the induction of apoptosis through a p53-mediated pathway. Pyknotic NPCs were distributed across the ventricular zone (VZ) of the telencephalic wall until 12 HAT, and became localized in the medial and dorsal layers at 12 and 48 HAT. Significant decreases in the numbers of mitotic NPCs and BrdU-LI% were noted from 3 HAT and 24 HAT, respectively. BrdU-positive NPCs were located in the ventral and middle layer at 24 and 48 HAT. p21-positive cells were detected at 12 and 24 HAT. The present results demonstrated that p53-mediated apoptosis was induced in all phases of the cell cycle of the NPCs in the early stage after 5-FU treatment. Furthermore, apoptosis of NPCs and suppression of cell proliferative activity are the events that take place in parallel leading to prominent reduction in the width of the telencephalic wall. (DOI: 10.1293/tox.2020-0070; J Toxicol Pathol 2021; 34: 299–308)

Key words: 5-Fluorouracil, time-course change, neural progenitor cell damage, histopathology, immunohistochemistry

Introduction

It is well known that 5-fluorouracil (5-Fu) inhibits DNA synthesis and perturbs the cell cycle through inhibition of thymidylate synthetase[1–4], and therefore, 5-Fu has been widely used as a cytostatic anti-tumor drug. In addition, 5-Fu is absorbed rapidly into the maternal circulation and its metabolites are directly incorporated into embryonic nucleic acid[5] resulting in the induction of teratogenic effects and subsequent developmental anomalies in the craniofacial tissues, limb buds, and brain in a number of animal species, including humans[2, 3, 6–9]. Hindlimb anomalies induced by 5-Fu have been studied in detail, and they are likely to be induced by prenatal damage to the cells composing the hindlimbs[2, 3]. However, 5-Fu has not been adequately investigated for its toxic effects on the developing fetal nervous system, although a number of DNA-damaging agents show toxic effects on the developing fetal brain of rats and mice[10]. Kumar *et al.*[11] reported that a single injection of 5-Fu into pregnant rats during the late phase of pregnancy brought about microencephaly in the prenatal and neonatal brain. In our previous study, the toxic effects of 5-Fu (15 to 50 mg/kg b.w.) were examined on rat fetuses after treatment on gestation day (GD) 13, and we demonstrated that in addition to mesenchymal cell damage in the craniofacial region, limb bud, and tongue, 5-Fu caused pyknosis and subsequent loss of neural progenitor cells (NPCs) in the fetal brain and spinal cord[12].

Since the rat fetus at GD13 is in the early neural developmental stage and very sensitive to DNA-damaging agents, a number of studies have focused on GD13 for DNA-damaging agent-induced lesions in the developing rat brain[10]. In the developing brain, multipotent NPCs proliferate in the VZ, and then differentiate into neurons and later, glial cells[13]. The nuclei of proliferating NPCs undergo a characteristic migration process (interkinetic nuclear migration or elevator movement) in the VZ, and their locations are well correlated with their cell cycle phase[14].

Taking these facts into consideration, the present study was designed to investigate the morphological and immunohistochemical changes in NPCs of the rat fetal brain over time from 3 to 72 h after treatment (HAT) to dams with 5-Fu on GD13. Particular interest was focused on the effect on the telencephalon wall because of its criticality in post-

Received: 3 October 2020, Accepted: 11 May 2021
Published online in J-STAGE: 3 June 2021
*Corresponding author: Y Yamaguchi
(e-mail: yamaguchi-yuko@bozo.co.jp)
©2021 The Japanese Society of Toxicologic Pathology
This is an open-access article distributed under the terms of the Creative Commons Attribution Non-Commercial No Derivatives (by-nc-nd) License. (CC-BY-NC-ND 4.0: https://creativecommons.org/licenses/by-nc-nd/4.0/).

natal microcephaly. In addition, the possible mechanism was investigated in comparison with the changes induced by other DNA-damaging agents.

Materials and Methods

Animals and experimental design

Forty-two pregnant rats of the Sprague-Dawley strain [Crl:CD(SD)] were obtained at GD7 from Charles River Japan Inc. (Tsukuba Breeding Center, Ibaraki, Japan). The day when copulation was confirmed was defined as GD0. Animals were housed individually in bracket-type stainless-steel wire mesh cages (W254 × D350 × H170 mm) and maintained in a barrier-sustained animal room controlled at 23 ± 3°C and 50 ± 20% relative humidity, with 10 to 15 times/h ventilation and 12h/12h light/dark cycle. Animals were allowed free access to radiation-sterilized pellets (NMF; Oriental Yeast Co., Ltd. Tokyo, Japan) and tap water *ad libitum*.

5-Fu (FUJIFILM Wako Pure Chemicals, Osaka, Japan) and 5-bromo-2'-deoxyuridine (BrdU) (Sigma-Aldrich Japan, Tokyo, Japan) was dissolved in sterile water and saline, respectively. The dose of 5-Fu used in the present study was determined based on the results of our previous study[12].

Forty-two pregnant rats were equally divided into the control and 5-Fu groups. On GD13, dams of the 5-Fu group were injected intraperitoneally (i.p.) with 50 mg/kg b.w. (10 mL/kg b.w.) of F-5u and those of the control group with 10 mL/kg b.w. of sterile water. Three randomly chosen dams of the control and 5-Fu groups each were euthanized at each time point of 3, 6, 9, 12, 24, 48, and 72 HAT by exsanguination from the abdominal aorta under inhalation anesthesia. All the dams were injected intravenously (i.v.) with 100 mg/kg b.w. (10 mL/kg b.w.) of BrdU 30 min before euthanasia to detect cells in the S-phase. At each time point, body weights were obtained for all fetuses per dam from 3 dams, and the brains of 3 randomly chosen fetuses from each dam were examined histopathologically and immunohistochemically.

All the procedures of this study were performed in accordance with the protocol approved by the Animal Care and Use Committee of BoZo Research Center Inc.

Histopathology

All fetuses were fixed in 10% neutral-buffered formalin, processed to paraffin-embedded blocks, sectioned at 2 μm, and stained with hematoxylin and eosin (HE) for histopathological examination of the brain. Their brains were also immunohistochemically analyzed as described below. In our previous study, damage to NPCs was primarily observed in the telencephalon as compared to the other regions of the diencephalon, mesencephalon, and metencephalon[12]. Therefore, emphasis was placed on the telencephalon, and the anterior region of the telencephalon wall (Fig. 1) was prominently examined in this study.

Immunohistochemistry

Paraffin sections were deparaffinized and immersed in 10 mM citrate buffer, pH 6.0, and heated at 120°C for 20 min in an autoclave. The sections were rinsed with Tris-buffered saline (TBS), and placed in methanol containing 0.3% H_2O_2 for 30 min to inactivate endogenous peroxidase. They were then incubated with TBS blocking buffer at room temperature for 30 min to prevent nonspecific staining. Immunohistochemistry for cleaved caspase-3 (for apoptotic cells), p53, p21, and BrdU was performed as described below.

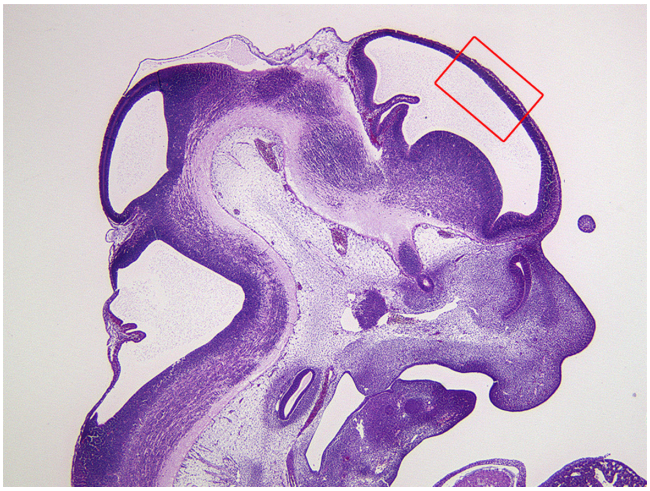

Fig. 1. Microscopic photograph of a transverse section of the brain of a normal fetal rat on GD13. HE staining. The telencephalic wall enclosed in a red frame was examined in the present study.

For NPCs positive to cleaved caspase-3, the sections were allowed to react with rabbit anti-cleaved caspase-3 polyclonal antibody (1:200, Cell Signaling Technology, Japan, Tokyo) at 4°C overnight and Envision+ kit (Dako Japan, Kyoto, Japan) at room temperature for 60 min. For p53- and p21-positive NPCs, a TSA Biotin System kit (PerkinElmer, Waltham, MA, USA) was used. In brief, the sections were allowed to react with rabbit anti-p53 polyclonal antibody (1:1000; Santa Cruz Biotechnology, Santa Cruz, CA, USA) or rabbit anti-p21 monoclonal antibody (1:100, Clone SX118, Dako Japan) at 4°C overnight. They were then incubated with biotinylated antibody against rabbit IgG (1:400, Dako Japan) for 40 min, with streptavidin-horseradish peroxidase (1:300, Dako Japan) for 40 min, with biotinyltyramide amplification reagent at room temperature for 10 min, and finally with streptavidin-HRP in TBS buffer at room temperature for 30 min. BrdU-positive cells were detected according to the following procedure. Endogenous peroxidase activity was blocked with 0.3% H_2O_2 in methanol for 30 min, and the sections were incubated with 2 N HCl at room temperature for 30 min, followed by 0.05% protease (Protease type XXIV, Sigma-Aldrich Japan) at room temperature for 5 min. Thereafter, they were allowed to react with mouse anti-BrdU monoclonal antibody (1:200, Dako Japan) at 4°C overnight and with the Envision+ kit (Dako Japan) at room temperature for 60 min.

Positive cells were visualized using peroxidase-diaminobenzidine (DAB, Dojindo Laboratories, Kumamoto,

Japan) reaction under counterstaining with methylgreen or hematoxylin.

Morphometry

At each time point in the investigation, pyknotic and mitotic NPCs were counted in the VZ of the telencephalic wall in 3 randomly chosen fetuses from 3 dams on HE-stained sections under a light microscope. The number of pyknotic NPCs was counted from 300 to 500 NPCs in the telencephalic wall, and the pyknosis index was calculated as the percentage of pyknotic cells out of the total number of NPCs counted. The number of mitotic NPCs was counted in the field of ×400 view. The number of NPCs positive for cleaved caspase-3, p53, p21, and BrdU and their labeling indices (LIs%) were counted in the same manner.

Statistical analysis

The fetal weights and LIs% of pyknotic and mitotic NPCs, and cleaved cappase-3-, p53-, p21-, and BrdU-positive NPCs were expressed as the mean ± standard deviation (SD). The fetal weights, mitotic NPCs, and cleaved caspase-3-, p53-, and BrdU-positive NPCs were compared between the 5-Fu and control groups at each tine point using the F-test, Student's *t*-test, and/or Welch's *t*-test. For all comparisons, p-values less than 5% ($p<0.05$) and 1% ($p<0.01$) were considered to be statistically significant.

Results

Clinical findings

No deaths occurred in dams or fetuses in any group at any of the examined time points, and all the litter sizes were within an expected range of variation. The fetal weights were significantly reduced in the 5-Fu group at 48 and 72 HAT as compared with the control group (Fig. 2).

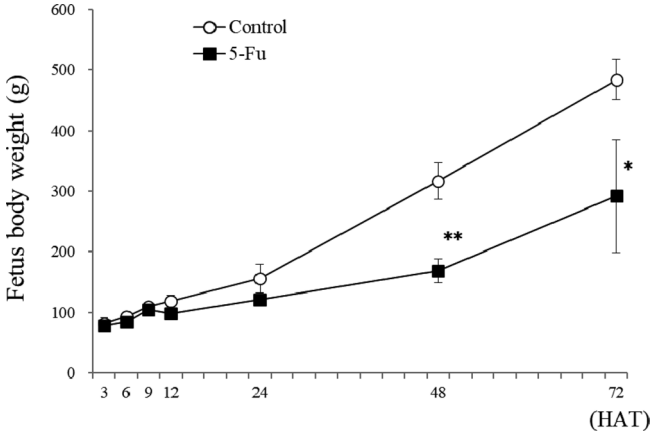

Fig. 2. Body weight changes in fetuses following treatment with 5-Fu. The body weight of fetuses in the 5-Fu group significantly reduced as compared to the control group from 48 HAT.

Histopathological and immunohistochemical findings

In the control group, pyknotic NPCs were scarce throughout the experimental period (Figs. 3a, 3i and 4). Cell kinetics of the pyknotic NPCs was of interest in the 5-Fu group. They were scattered across the VZ at 6 HAT (Fig. 3c), progressively increased throughout all layers of the VZ at 9 (Fig. 3d) and 12 HAT (Fig. 3e) and thereafter, found in the medial and dorsal layers of the VZ at 24 (Fig. 3f) and 48 HAT (Fig. 3g), and at the end, obviously decreased at 72 HAT (Fig. 3h). At 72 HAT, the width of the telencephalic wall was prominently reduced in the 5-Fu group because of lack of the subventricular zone (Fig. 3i). The pyknotic NPC index increased at 9 HAT, peaked at 12 HAT, and decreased gradually thereafter (Fig. 4). The pyknotic NPCs were positive for cleaved caspase-3 (Fig. 5), and over time, the cleaved caspase-3-LI% (Fig. 6) correlated well with the pyknotic index.

Although mitotic NPCs were observed in the ventricular surface of the VZ in the control group (Fig. 3a and 3i), the number of mitotic NPCs was significantly reduced in the 5-Fu group at all time points (Fig. 7).

There were no p53-positive NPCs in the telencephalic wall throughout the experimental period in the control group. In the 5-Fu group, numerous p53-positive NPCs were observed throughout the VZ at 3 HAT (Fig. 8b) when the p53-LI% reached its maximal level (Fig. 9). The p53-positive NPCs were still present and intermingled with the pyknotic NPCs throughout the VZ at 12 HAT (Fig. 8c) when the pyknotic NPCs index reached its peak level. They returned to the level close to the control value (Fig. 9).

In the 5-Fu group, p21-positive NPCs were detected at 12 and 24 HAT, with a higher p21-LI% than the control group (Figs. 10 and 11).

For BrdU immunohistochemistry, BrdU-positive NPCs were observed in the dorsal layer of the VZ where S-phase NPCs are usually located, except at 24 HAT in the control group (Fig. 12a–f), whereas many BrdU-positive NPCs were found together with pyknotic cells in the dorsal and medial layers until 12 HAT (Fig. 12g-i), and shifted to the ventral layer of the VZ (Fig. 12j and 12k) and dorsal layer (Fig. 12I) at 24/48 and 72 HAT, respectively, in the 5-Fu group. The BrdU-LI% significantly decreased at 24 and 48 HAT; however, it returned to the control level at 72 HAT (Fig. 13).

Discussion

In the present study, the fetal weights were reduced in the 5-Fu group at 48 and 72 HAT as compared with the control group. Our previous study also revealed similar decreases in the fetal weights after treatment of 5-FU on GD 13, in addition to prominent pyknosis in mesenchymal cells of the craniofacial region, limb bud, tongue, and central nervous system[12]. The degree of pyknosis in NPCs progressed prominently in all the layers of the VZ at 9 HAT and pyknotic NPCs were positive for cleaved caspase-3, indicating that the damage to NPCs caused the onset of decreased fetal weights. Therefore, the observed decrease in fetal weights is

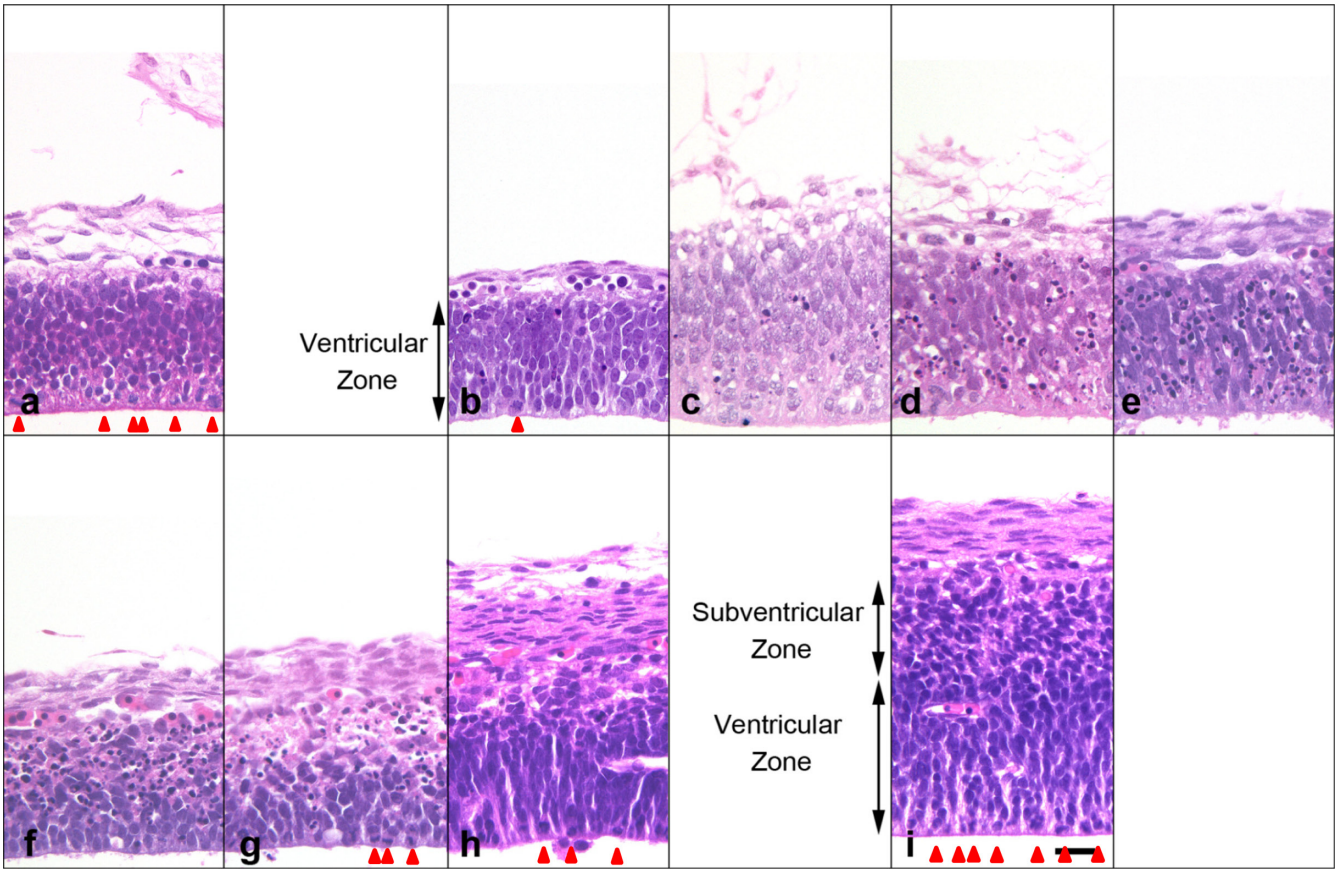

Fig. 3. Histopathological changes of the telencephalic wall of fetal rats in the control group at 3 (a) and 72 HAT (i), and 5-Fu group at 3 (b), 6 (c), 9 (d), 12 (e), 24 (f), 48 (g), and 72 HAT (h). In the 5-Fu group, pyknotic NPCs are scattered throughout the VZ at 6 HAT, however, they show prominent increases in numbers in all the layers at 9 and 12 HAT. These pyknotic NPCs are exclusively localized to the medial and dorsal layers at 24 and 48 HAT. The pyknotic NPCs are not visible anymore and the width of telencephalic wall is prominently reduced at 72 HAT. Mitotic NPCs (red arrow heads) are absent or decreased in the 5-Fu group. HE. Bar: 20 μm.

likely to be attributable in part to the developmental disorders related to the loss of NPCs in the brain.

A number of findings were observed in NPCs of the telencephalic wall of the brain in fetal rats after intraperitoneal injection to dams with 5-Fu on GD13. The pyknotic NPCs were positive for cleaved caspase-3, a marker of apoptotic cells, and the pyknotic and cleaved caspase-3-LI% showed parallel time-course changes, indicating that 5-Fu induced apoptosis in NPCs in the fetal brain. The p53-LI% reached its maximal level at 3 HAT when apoptotic NPCs were not yet evident, and maintained a high level until 12 HAT when the apoptotic index reached its peak. p53 plays a crucial role in DNA repair, cell cycle arrest, and apoptosis in response to DNA damage[15, 16]. p53 activated by DNA damage initiates cell death by stimulating the death receptors and Bax in the mitochondrial membrane leading to caspase-3 activation before the induction of apoptosis[17]. Therefore, it was strongly suggested that 5-Fu induces apoptosis of NPCs through a p53-mediated pathway, in a manner similar to that of a number of DNA-damaging agents[10].

The peak time of the number of apoptotic and mitotic NPCs and the distribution of apoptotic NPCs in the

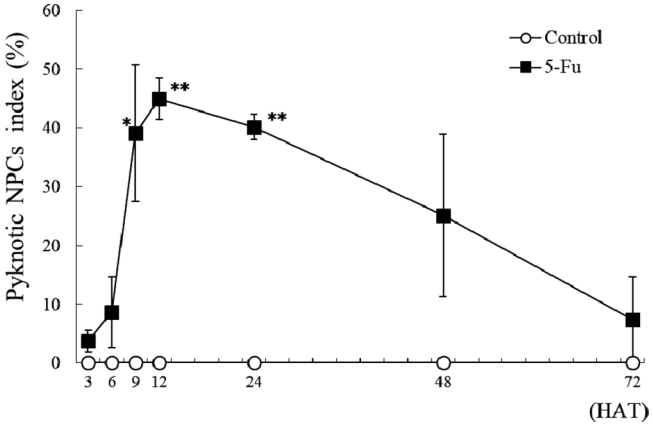

Fig. 4. Changes in the pyknotic NPC index in the telencephalic wall. In the 5-Fu group, the index increases at 9 HAT, peaks at 12 HAT, and returns close to the control level at 72 HAT. Each value represents the mean ± SD of 3 dams. *$p<0.05$ and **$p<0.01$.

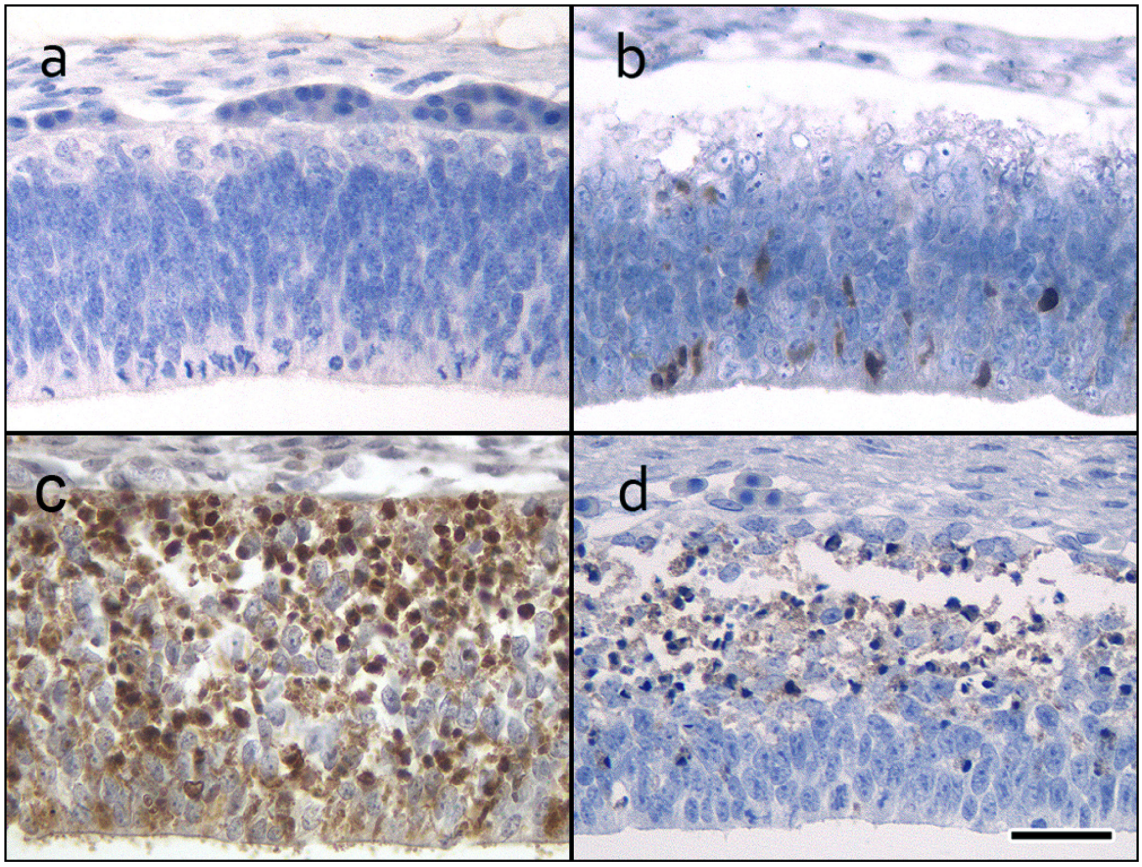

Fig. 5. Immunohistochemical expression of cleaved caspase-3 in the telencephalic wall of fetal rats in the control group at 12 HAT (a), and 5-Fu group at 6 (b), 12 (c), and 48 HAT (d). In the 5-Fu group, a small number of positive NPCs are scattered throughout the VZ at 6 HAT and numerous positive NPCs are observed throughout the VZ at 12 HAT. These positive cells are found in the middle and dorsal layers of the VZ at 48 HAT. Immunostaining. Bar: 30 μm.

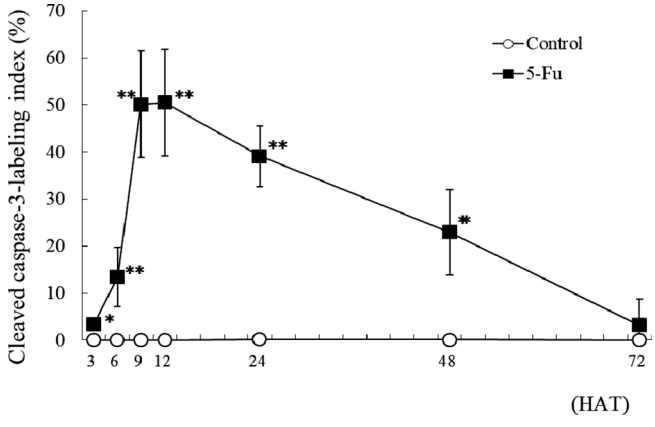

Fig. 6. Changes in the cleaved caspase-3-labeling index in the telencephalic wall. In the 5-Fu group, the index increases at 3 HAT, peaks at 9 and 12 HAT, and returns close to the control level at 72 HAT. Changes in the cleaved caspase-3-labeling index correlate well to those in the pyknotic NPC index (Fig. 3). Each value represents the mean ± SD of 3 dams. *p<0.05 and **p<0.01.

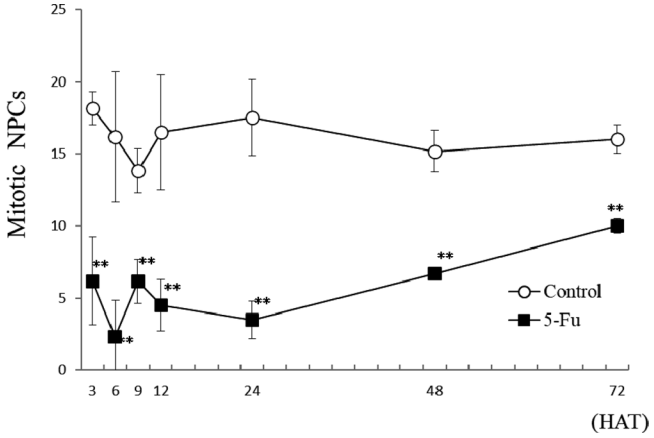

Fig. 7. Changes in the number of mitotic NPCs in the telencephalic wall. In the 5-Fu group, the number of mitotic NPCs significantly decreases at all time points. Each value represents the mean ± SD of 3 dams. *p<0.05 and **p<0.01.

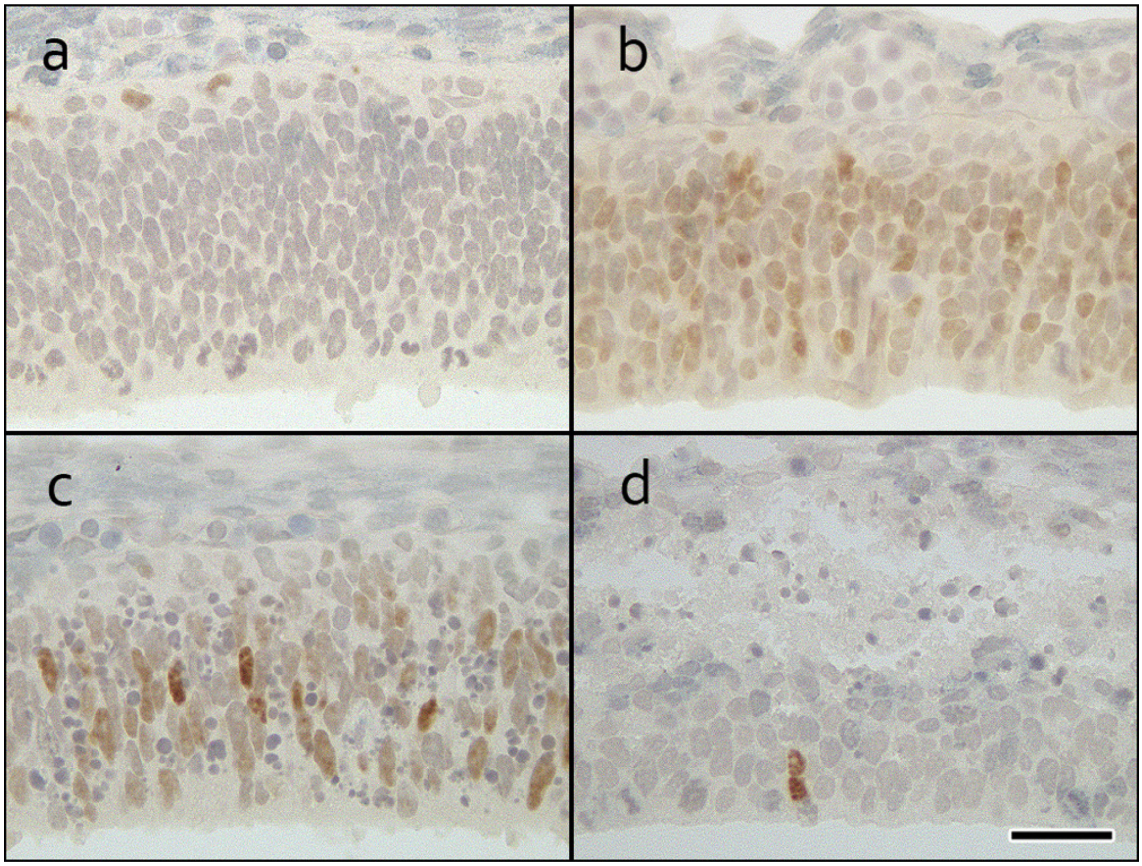

Fig. 8. Immunohistochemical expression of p53 in the telencephalic wall of fetal rats in the control group at 3 HAT (a), and 5-Fu group at 3 (b), 12 (c), and 48 HAT (d). In the 5-Fu group, numerous positive NPCs are observed in the VZ at 3 HAT. The number of positive NPCs decreases at 12 HAT and only a few positive cells are observed at 48 HAT. Immunostaining. Bar: 30 μm.

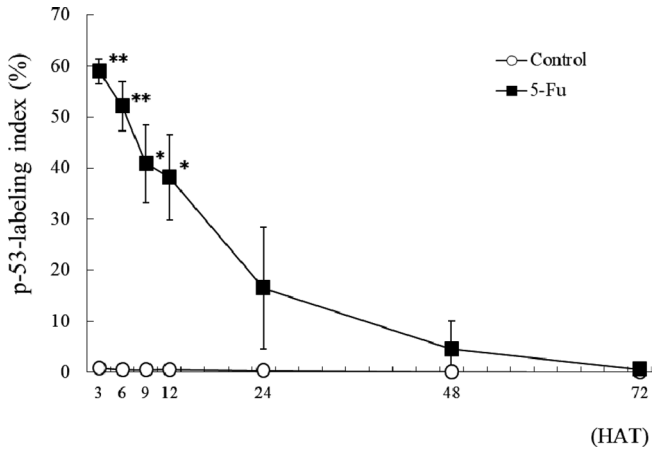

Fig. 9. Changes in the p53-labeling index in the telencephalic wall. In the 5-Fu group, the index shows a maximal level at 3 HAT. Thereafter, it decreases gradually and returns to the control level at 72 HAT. Each value represents the mean ± SD of 3 dams. *p<0.05 and **p<0.01.

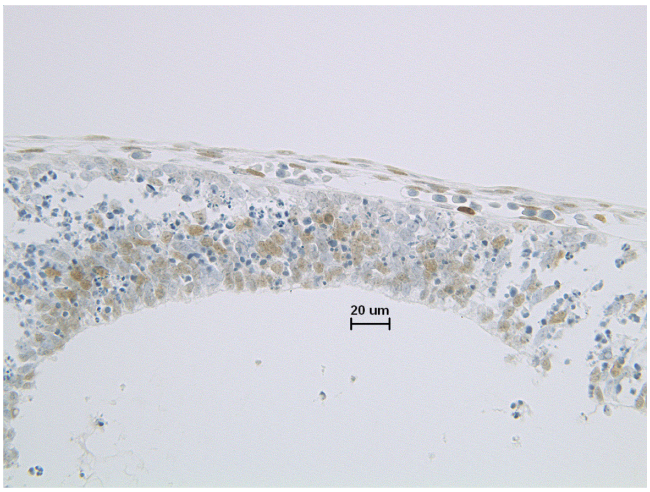

Fig. 10. Immunohistochemical expression of p21 in the telencephalic wall of the fetal rats in the 5-Fu group at 24 HAT. Numerous positive NPCs are visible in all layers of the VZ.

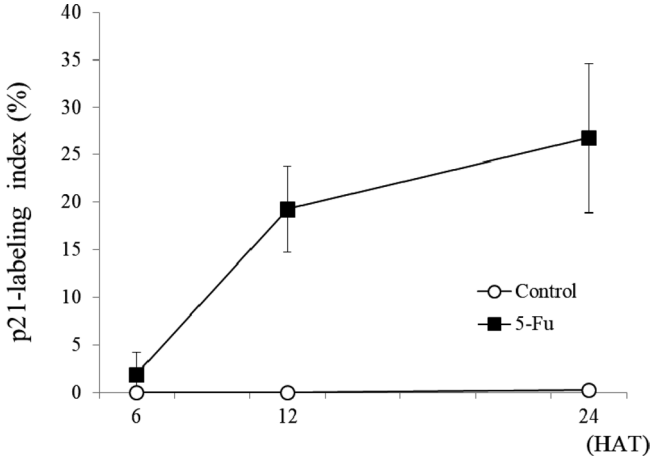

Fig. 11. Changes in the p21-labeling index in the telencephalic wall. In the 5-Fu group, the index shows a gradual increase at 12 and 24 HAT. Each value represents the mean ± SD of 3 dams.

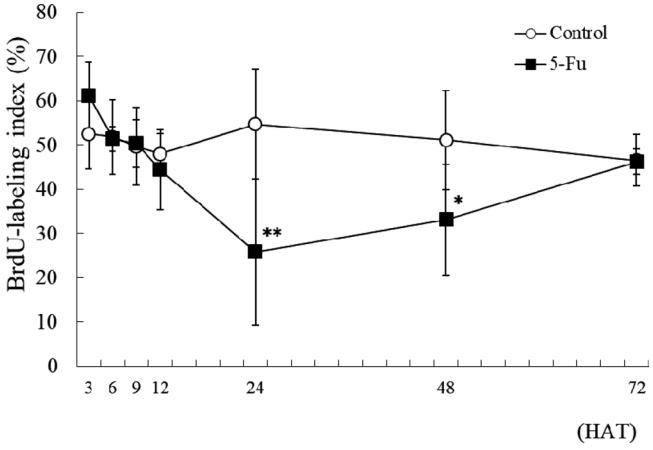

Fig. 13. Changes in the BrdU-labeling index in the telencephalic wall. In the 5-Fu group, the index shows a significant decrease at 24 and 48 HAT, and returns to the control level at 72 HAT. Each value represents the mean ± SD of 3 dams. *p<0.05 and **p<0.01.

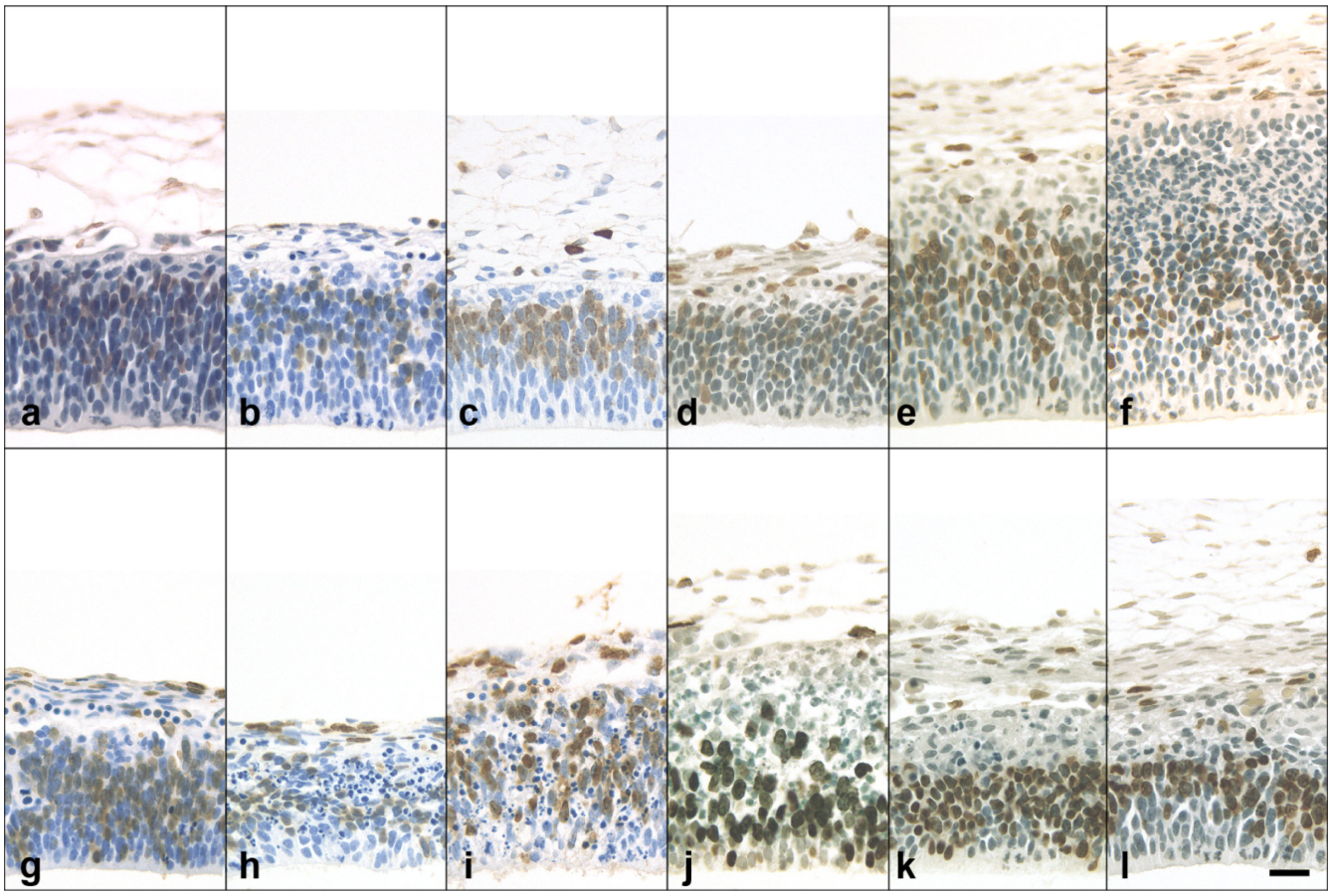

Fig. 12. Immunohistochemical expression of BrdU in the telencephalic wall of fetal rats in the control group at 3 HAT (a), 9 (b), 12 (c), 24 (d), 48 (e), and 72 HAT (f), and 5-Fu group at 3 (g), 9 (h), 12 (i), 24 (j), 48 (k), and 72 HAT (l). BrdU-positive NPCs are observed in the dorsal layer of the VZ where S-phase NPCs are located, except at 24 HAT in the control group. In the 5-Fu group, many BrdU-positive NPCs are found in the dorsal and medial layer with pyknotic cells until at 12 HAT. At 24 and 48 HAT, they aggregate in the ventral layer.

VZ of the telencephalic wall vary among DNA-damaging agents, including ethylnitrosourea[18], cytosine arabinoside[19], hydroxyurea[20], 6-mercaptopurine[21], etoposide[22], and 5-azacytidine[23]. Such variations are considered to reflect the differences in pharmacokinetics, mechanisms of action of DNA damage, signaling pathways involved in apoptosis, and cell cycle arrest among these DNA-damaging agents[10, 24, 25]. Doi reported that the number of apoptotic NPCs peaks at 9 to 12 HAT with DNA damaging agents such as ENU, hydroxyurea, 5-azacytidine, and cytosine arabinoside[10]. In the present study, the pyknotic and apoptotic NPC indices increased at 9 HAT, and peaked at 12 HAT in the 5-Fu group. The points of p53 expression prior to the occurrence of the apoptosis induced by 5-Fu were similar to those of ENU-induced apoptosis. Therefore, there might be some similarities in the possible mechanism of apoptosis between the DNA-damaging agents described above and 5-FU.

The 5-Fu-induced apoptotic NPCs first appeared across the VZ during the early stage of the study, then shifted to the middle and dorsal layers at 24 and 48 HAT, and finally disappeared from the VZ at 72 HAT. The distribution of the 5-Fu-induced apoptotic NPCs during the early stage (3 to 12 HAT) was similar to that induced by intraperitoneal exposure of methotrexate (MTX)[26]. It is well known that the positions of NPC nuclei are correlated with their cell cycle phase (Fig. 14); S-phase nuclei are located in the dorsal layer of the VZ, and then migrate inward during the G2 phase, followed by mitosis at the ventricular surface[10]. The nuclei then migrate outward during the G1 phase and enter the S phase again in the dorsal layer of the VZ. Sun *et al.* suggested that MTX induces apoptosis of NPCs in all phases of the cell cycle and this apoptosis occurs independently of cell cycle arrest[26]. Considering these facts together with our findings, it is conceivable that 5-Fu likely induces apoptosis of NPCs in all phases of the cell cycle during the early stage of dosing. A question thus arises as to why S-phase cells were located in the ventral layer, but no evidence to clarify the meaning of such a finding was obtained in the present study. However, we found that the numbers of mitotic cells was still low and apoptotic cells were aggregated in the dorsal layer at 24 and 48 HAT. These findings suggest that G2 and M phase cells which are normally present in the ventral and middle layer did not recover from the severe cell damage in the early stage of 5-FU administration, and the S-phase cells in the dorsal layer were still affected by 5-Fu. Therefore, S-phase NPCs that migrated from the surviving G1-phase NPCs and arrested from 12 HAT are likely to be located in the ventral layer.

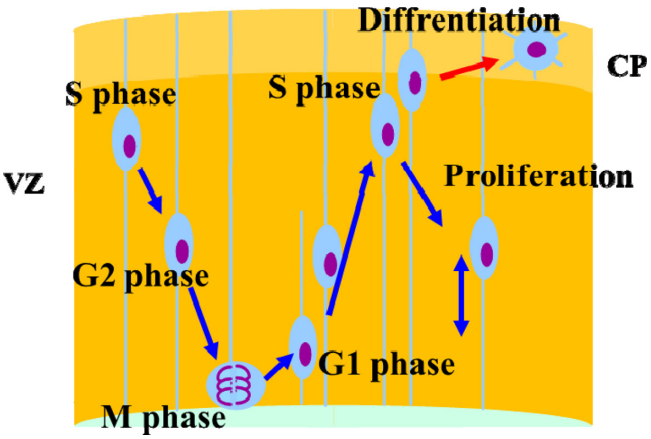

Fig. 14. Nuclear migration and cell cycle phase of NPCs in the VZ of the telencephalic wall. The proliferating NPCs undergo a characteristic migration in the VZ, in which the positions of the nuclei are correlated with their cell cycle phase. CP: Cortical plate.

Following 5-Fu treatment, significant decreases in the numbers of mitotic NPCs and BrdU-LI% were noted from 3 HAT and 24 HAT respectively, while the cleaved caspase-3-LI% increased significantly from 3 to 48 HAT. These changes indicated that cell proliferative activity was suppressed during the period when marked apoptosis developed in the VZ. The apoptotic NPCs were localized in the dorsal layer where S-phase cells normally exist, whereas the BrdU-positive NPCs were primarily observed in the ventral and middle layers at 24 and 48 HAT when mitotic NPCs reappeared at the ventricular surface of the VZ. Since the positions of NPC nuclei are reportedly correlated with their cell cycle phase[10], their detection in the ventral layer at 48 HAT in our study suggested that S-phase NPCs which probably survived from the 5-Fu-induced damage aggregated in the ventral layer.

The p21-LI% significantly increased at 12 and 24 HAT (Fig. 11). p21 is a potent cyclin-dependent kinase inhibitor and functions as a regulator of cell cycle progression in S and G1 phases[27]. Expression of the p21 gene is tightly regulated by p53[17], wherein p53 transactivates p21 and other target genes resulting in suppression of the cell proliferative activity before apoptotic cell death and cell cycle arrest[28]. 5-Fu induces cell cycle arrest at the G1/S phase in mouse embryonic stem cells[29]. In the present study, detection of BrdU-positive cells in the ventral and middle zones at 24 and 48 HAT suggests that G1-S arrest occurred in NPCs which survived from the 5-Fu-induced damage in the ventral layer. Since the DNA damage induced by 5-Fu at 50 mg/kg was too severe for the fetal NPCs to repair, it is conceivable that such critical DNA damage not only activates p53 to initiate apoptosis in the early stage, but also results in G1-S arrest due to the suppressed DNA repair function in the late stage of the 24-hour timeframe after 5-Fu treatment.

There have been several reports demonstrating that 5-Fu is capable of inducing cell cycle arrest at the G1/S phase in rat embryonic hindlimb[21] and mouse embryonic stem cells[29], and at the G2/M phase in keloid fibroblasts[30]. Another report described that DNA damage results in an increase in cell cycle arrest at G1 and/or G2 phases, reduced rates of DNA synthesis, and finally, apoptosis[31]. In the present study, although flow cytometric analysis on cell cycle and western blot analysis on cell cycle-related proteins were not conducted, the following findings were obtained in the 5-Fu group: the number of mitotic NPCs was significantly

reduced throughout the observation period, and the distribution kinetics of the apoptotic NPCs induced by 5-Fu after 24 HAT was similar to that induced by 6-mercaptopurine[21, 32] and etoposide[22, 33], inducing cell cycle arrest at G2/M. Therefore, all the above mentioned findings suggest that 5-Fu also induces cell cycle arrest at G2/M.

At 72 HAT, all the morphometric values except the mitosis index were comparable to the control group, suggesting that the DNA damage induced by 5-Fu at 50 mg/kg entered the recovery phase. At the end of the experimental period, the width of the telencephalic wall was prominently reduced due to excessive cell loss resulting from marked apoptotic cell death and the subventricular zone was not developed in the 5-Fu group. However, the cerebral cortex in the newborn rats administrated 5-Fu (40 mg/kg, at GD18) displayed neither apoptosis nor abnormal structures (data not shown). Apoptosis of embryonic cells induced by teratogens is one of the most important events proceeding abnormal development[34]. The results of our study further suggest that the neonatal malformation of the brain associated with 5-Fu treatment is largely dependent on the severity of DNA damage occurring in the critical period of exposure during brain development.

In conclusion, the present results demonstrated that p53-mediated apoptosis was induced in NPCs at all cell cycle across all layers of the VZ during the early stage after 5-Fu treatment and suggested that S-phase NPCs aggregate in the ventral layer due to G1-S arrest in the later stage. Furthermore, it was confirmed that apoptosis of NPCs and suppression of cell proliferation activity occur in parallel, leading to prominent reduction in the width of the telencephalic wall. Further studies are needed to clarify the effects of 5-Fu on the cell cycle of NPCs in the fetal rat brain.

Disclosure of Potential Conflicts of Interest: The authors have no conflicts of interest directly relevant to the content of this article.

Acknowledgements: The authors thank Dr. Kunio Doi, Professor Emeritus of the University of Tokyo, for critical review of this manuscript and Mr. Pete Aughton, D.A.B.T., ITR Laboratories Canada, for English language editing.

References

1. Pinedo HM, and Peters GF. Fluorouracil: biochemistry and pharmacology. J Clin Oncol. **6**: 1653–1664. 1988. [Medline] [CrossRef]
2. Shuey DL, Lau C, Logsdon TR, Zucker RM, Elstein KH, Narotsky MG, Setzer RW, Kavlock RJ, and Rogers JM. Biologically based dose-response modeling in developmental toxicology: biochemical and cellular sequelae of 5-fluorouracil exposure in the developing rat. Toxicol Appl Pharmacol. **126**: 129–144. 1994. [Medline] [CrossRef]
3. Shuey DL, Setzer RW, Lau C, Zucker RM, Elstein KH, Narotsky MG, Kavlock RJ, and Rogers JM. Biological modeling of 5-fluorouracil developmental toxicity. Toxicology. **102**: 207–213. 1995. [Medline] [CrossRef]
4. Elstein KH, Zucker RM, Andrews JE, Ebron-McCoy M, Shuey DL, and Rogers JM. Effects of developmental stage and tissue type on embryo/fetal DNA distributions and 5-fluorouracil-induced cell-cycle perturbations. Teratology. **48**: 355–363. 1993. [Medline] [CrossRef]
5. Inoue T, and Horii I. Effects on fetal thymocyte populations and postnatal T-cell-dependent immune functions after maternal exposure to 5-fluorouracil during pregnancy in mice. J Toxicol Sci. **27**: 79–86. 2002. [Medline] [CrossRef]
6. Lau C, Mole ML, Copeland MF, Rogers JM, Kavlock RJ, Shuey DL, Cameron AM, Ellis DH, Logsdon TR, Merriman J, and Setzer RW. Toward a biologically based dose-response model for developmental toxicity of 5-fluorouracil in the rat: acquisition of experimental data. Toxicol Sci. **59**: 37–48. 2001. [Medline] [CrossRef]
7. Paskulin GA, Gazzola Zen PR, de Camargo Pinto LL, Rosa R, and Graziadio C. Combined chemotherapy and teratogenicity. Birth Defects Res A Clin Mol Teratol. **73**: 634–637. 2005. [Medline] [CrossRef]
8. Hanaoka H, Kubota T, Matsui K, Kadokura Y, Iida M, Yamada Y, and Moteki H. A case of leukoencephalopathy after drip infusion of 5-fluoroirasil. Pract Odontol. **109**(Suppl): 161–163. 2002 (in Japanese).
9. Leyder M, Laubach M, Breugelmans M, Keymolen K, De Greve J, and Foulon W. Specific congenital malformations after exposure to cyclophosphamide, epirubicin and 5-fluorouracil during the first trimester of pregnancy. Gynecol Obstet Invest. **71**: 141–144. 2011. [Medline] [CrossRef]
10. Doi K. Mechanisms of neurotoxicity induced in the developing brain of mice and rats by DNA-damaging chemicals. J Toxicol Sci. **36**: 695–712. 2011. [Medline] [CrossRef]
11. Kumar S, Lobo SW, Dubey AK, and Pandey SK. Teratogenic effects of 5-fluorouracil on rat brain. Nepal Med Coll J. **8**: 7–8. 2006. [Medline]
12. Yamaguchi Y, Aoki A, Fukunaga Y, Matsushima K, Ebata T, Ikeya M, and Tamura K. 5-fluorouracil-induced histopathological changes in the central nervous system of rat fetuses. Histol Histopathol. **24**: 133–139. 2009. [Medline]
13. Temple S. The development of neural stem cells. Nature. **414**: 112–117. 2001. [Medline] [CrossRef]
14. Ueno M, Katayama K, Yamauchi H, Nakayama H, and Doi K. Cell cycle progression is required for nuclear migration of neural progenitor cells. Brain Res. **1088**: 57–67. 2006. [Medline] [CrossRef]
15. Uberti D, Belloni M, Grilli M, Spano P, and Memo M. Induction of tumour-suppressor phosphoprotein p53 in the apoptosis of cultured rat cerebellar neurones triggered by excitatory amino acids. Eur J Neurosci. **10**: 246–254. 1998. [Medline] [CrossRef]
16. Lakin ND, and Jackson SP. Regulation of p53 in response to DNA damage. Oncogene. **18**: 7644–7655. 1999. [Medline] [CrossRef]
17. Zhang XP, Liu F, and Wang W. Coordination between cell cycle progression and cell fate decision by the p53 and E2F1 pathways in response to DNA damage. J Biol Chem. **285**: 31571–31580. 2010. [Medline] [CrossRef]
18. Katayama K, Ishigami N, Uetsuka K, Nakayama H, and Doi K. Ethylnitrosourea (ENU)-induced apoptosis in the rat fetal tissues. Histol Histopathol. **15**: 707–711. 2000. [Medline]
19. Yamauchi H, Katayama K, Yasoshima A, Uetsuka K, Na-

kayama H, and Doi K. 1-β-D-Arabinofuranosylcytosine (Ara-C)-induced apoptosis in the rat fetal tissues and placenta. J Toxicol Pathol. **16**: 223–229. 2003. [CrossRef]
20. Woo GH, Bak EJ, Nakayama H, and Doi K. Molecular mechanisms of hydroxyurea(HU)-induced apoptosis in the mouse fetal brain. Neurotoxicol Teratol. **28**: 125–134. 2006. [Medline] [CrossRef]
21. Kanemitsu H, Yamauchi H, Komatsu M, Yamamoto S, Okazaki S, and Nakayama H. Time-course changes in neural cell apoptosis in the rat fetal brain from dams treated with 6-mercaptopurine (6-MP). Histol Histopathol. **24**: 317–324. 2009. [Medline]
22. Nam C, Woo GH, Uetsuka K, Nakayama H, and Doi K. Histopathological changes in the brain of mouse fetuses by etoposide-administration. Histol Histopathol. **21**: 257–263. 2006. [Medline]
23. Ueno M, Katayama K, Yasoshima A, Nakayama H, and Doi K. 5-Azacytidine (5AzC)-induced histopathological changes in the central nervous system of rat fetuses. Exp Toxicol Pathol. **54**: 91–96. 2002. [Medline] [CrossRef]
24. Yamauchi H, Katayama K, Ueno M, Uetsuka K, Nakayama H, and Doi K. Involvement of p53 in 1-beta-D-arabinofuranosylcytosine-induced rat fetal brain lesions. Neurotoxicol Teratol. **26**: 579–586. 2004. [Medline] [CrossRef]
25. Katayama K, Uetsuka K, Ishigami N, Nakayama H, and Doi K. Apoptotic cell death and cell proliferative activity in the rat fetal central nervous system from dams administered with ethylnitrosourea (ENU). Histol Histopathol. **16**: 79–85. 2001. [Medline]
26. Sun J, Sugiyama A, Inoue S, Takeuchi T, and Furukawa S. Effect of methotrexate on neuroepithelium in the rat fetal brain. J Vet Med Sci. **76**: 347–354. 2014. [Medline] [CrossRef]
27. el-Deiry WS, Tokino T, Velculescu VE, Levy DB, Parsons R, Trent JM, Lin D, Mercer WE, Kinzler KW, and Vogelstein B. WAF1, a potential mediator of p53 tumor suppression. Cell. **75**: 817–825. 1993. [Medline] [CrossRef]
28. Levine AJ. p53, the cellular gatekeeper for growth and division. Cell. **88**: 323–331. 1997. [Medline] [CrossRef]
29. Kim GD, Rhee GS, Chung HM, Chee KM, and Kim GJ. Cytotoxicity of 5-fluorouracil: Effect on endothelial differentiation via cell cycle inhibition in mouse embryonic stem cells. Toxicol In Vitro. **23**: 719–727. 2009. [Medline] [CrossRef]
30. Huang L, Wong YP, Cai YJ, Lung I, Leung CS, and Burd A. Low-dose 5-fluorouracil induces cell cycle G2 arrest and apoptosis in keloid fibroblasts. Br J Dermatol. **163**: 1181–1185. 2010. [Medline] [CrossRef]
31. Zhou BB, and Elledge SJ. The DNA damage response: putting checkpoints in perspective. Nature. **408**: 433–439. 2000. [Medline] [CrossRef]
32. Kanemitsu H, Yamauchi H, Komatsu M, Yamamoto S, Okazaki S, Uchida K, and Nakayama H. 6-Mercaptopurine (6-MP) induces cell cycle arrest and apoptosis of neural progenitor cells in the developing fetal rat brain. Neurotoxicol Teratol. **31**: 104–109. 2009. [Medline] [CrossRef]
33. Nam C, Doi K, and Nakayama H. Etoposide induces G2/M arrest and apoptosis in neural progenitor cells via DNA damage and an ATM/p53-related pathway. Histol Histopathol. **25**: 485–493. 2010. [Medline]
34. Brill A, Torchinsky A, Carp H, and Toder V. The role of apoptosis in normal and abnormal embryonic development. J Assist Reprod Genet. **16**: 512–519. 1999. [Medline] [CrossRef]